Materials and Structures, 1993, **26**, 74–89

Compressive-force path and behaviour of prestressed concrete beams

S. M. SERAJ, M. D. KOTSOVOS*, M. N. PAVLOVIĆ

*Department of Civil Engineering, Imperial College of Science, Technology and Medicine, University of London, London SW7 2BU, UK and *National Technical University of Athens, Greece*

A study of the performance of prestressed concrete beams designed either by conventional design methods or to a physical model proposed in compliance with the 'compressive-force path' concept is presented. Results obtained from testing heavily prestressed beams are reported, which show that members designed to the latter concept may be safer than their Code counterparts. The behaviour of these beams has been compared with similar prestressed concrete beams (also designed either to current code provisions or to the proposed method) – but subjected to a smaller amount of prestressing – in an effort to monitor the effect of the level of prestressing on the behaviour of members designed by different methods. In contrast to the current way of thinking, it emerges that an additional amount of prestressing, instead of increasing the shear contribution of concrete, may, in fact, limit the load-bearing capacity of the member itself.

NOTATION

A_s	Area of longitudinal tension reinforcement which continues for a distance at least equal to d beyond section being considered
A_{sv}	Area of transverse reinforcement
b_1	Effective width (see Fig. A1)
C	Compressive force in concrete
d	Effective depth (mm)
f_{cu}	Uniaxial compressive cube strength of concrete
f_{cyl}	Uniaxial cylinder strength
f_u	Ultimate stress of tension steel (N mm^{-2})
f_y	Yield stress of tension steel (N mm^{-2})
f_{yv}	Yield stress of stirrup material (N mm^{-2})
h	Horizontal projection of inclined portion of compressive-force path
M_c	Moment corresponding to failure load (N mm)
M_f	Flexural capacity (N mm)
P_e	Effective prestressing force in tendons
P_i	Initial prestressing force in tendons
R	Reaction at support
s	Distance from support of cross-section at which M_c is calculated (mm), equal to shear span for point loading and $2d$ (in reinforced concrete members) or h (in prestressed concrete members) for uniformly distributed loading
T	Tensile force in longitudinal steel
T_{sv}	Transverse tensile force
V_a	Applied shear force
V_c	Tensile force resisted by concrete alone in region where compressive-force path changes direction
X	Depth of neutral axis
x'	Depth of neutral axis considering triaxial conditions
X_g	Centroidal distance of uncracked concrete from compression face
z	Lever-arm distance
Δz	Increase in lever arm
ϕ	Bar size
ρ_w	Tension steel ratio (A_s/bd)
σ'_c	Nominal triaxial compressive stress
σ_c	$0.8f_{cyl}$
σ_{conf}	Confining pressure required for σ_c to increase to σ'_c
σ_t	Transverse tensile stress

0025-5432/93 © RILEM

1. INTRODUCTION

It can be argued that the design procedures for concrete structures should be based on realistic physical models and not solely on empirical equations, as rational models enable engineers to develop a better understanding of the actual structural behaviour. In this regard, the unsatisfactory nature of the shear design provisions of the present codes [1–4] becomes apparent from their collection of complex, restrictive empirical equations. It would appear that it is due to a general lack of understanding at the material level that the design procedures for structural concrete put forward by the current codes are unnecessarily complicated and do not always yield safe design solutions.

Early design procedures for reinforced concrete (RC) members in shear were based on the truss-analogy theory developed at the turn of the century by Ritter [5] and Mörsch [6]; and, now, nearly a century later, the traditional methods of RC design remain largely unchanged. This theory, which assumes that concrete is not capable of resisting tension, postulates that a cracked RC beam (Fig. 1) acts as a truss with parallel longitudinal chords, and with a web composed of diagonal concrete struts and transverse steel ties. When shear is applied to

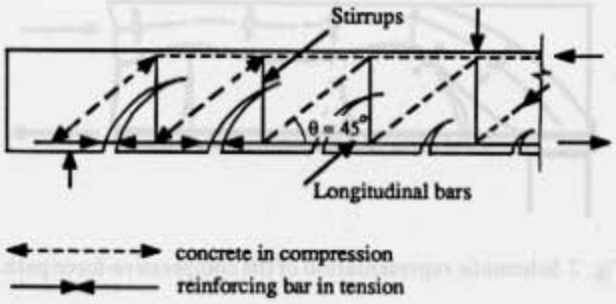

Fig. 1 Truss model.

this truss, the diagonal struts go into compression while tension is produced in the transverse ties and in the longitudinal bottom chord. In the most common form of this model, the crack angle θ formed between the longitudinal axis of the member and the diagonal compressive strut is assumed to be 45°.

Experience with the traditional 45° truss analogy having revealed the very conservative nature of the theory, present codes adopt this truss model in design practice after adding an empirical correction term, namely the 'concrete contribution', to the 45° truss equations. As prestressing increases the diagonal cracking load, the effects of prestress in a prestressed concrete (PSC) member are accounted for in the code equations by increasing the 'concrete contribution'. Present codes consider that the latter consists of the shear resistance of three separate components, namely (a) shear resistance of the compressive zone, (b) shear resistance due to aggregate interlock, and (c) shear resistance due to dowel action of the longitudinal reinforcement. In this respect, current codes are generally based on the view that the major contribution to shear resistance in beams without shear reinforcement is provided by the region of the beam below the neutral axis through the mechanisms (b) and (c) mentioned above. However, over the last few years it has been argued that, in contrast to these widely held views, the shear resistance of RC beams is in fact provided by the region of the path along which the compressive force is transmitted to the supports, rather than the region of the beam below the neutral axis [7,8].

The shear capacity of an RC beam is widely defined as the maximum shear force that can be sustained by a critical cross-section, with shear reinforcement being provided in order to carry that portion of the shear force that cannot be sustained by concrete alone. A precondition for the application of this 'shear capacity of critical sections' concept in design appears to be (by implication) the widely accepted view that the main contributor to shear resistance is the residual strength of 'cracked' concrete below the neutral axis described by the strain–softening characteristics of the material in tension and affected by 'aggregate interlock' [9–11]. This is because only through aggregate interlock can the cracked section below the neutral axis (the 'web' in the case of a T-beam) be the major contributor to the shear resistance of an RC or PSC member, as specified by current code provisions. Besides, the concept of the 'shear capacity of critical sections' is itself a prerequisite for the application of the 'truss analogy' since it is the loss of the shear capacity below the neutral axis that the shear reinforcement is considered to counterbalance. Recent test results [12–15], however, clearly raise doubts over generally accepted views, and indicate that 'truss' behaviour is not a necessary condition for reinforced or prestressed beams to attain their flexural capacity once their 'shear capacity' is exceeded. Evidently, a new model is needed for a rational explanation of the shear-transfer mechanism in RC and PSC members, and this proposition is strengthened by the outcome of numerical experiments which point to the conclusion that aggregate interlock plays a negligible role in such transfer mechanisms [16].

Although new concepts (e.g. compression field theory [17], modified compression field theory [18] and the strut-and-tie model [19]) have recently evolved in the general field of structural concrete design – with claims of far-reaching potential – most of these deviate very little from the basis on which present-day design is founded; and, thus, they carry implicit assumptions which, in many cases, are incompatible with the fundamental properties of concrete. The concept of 'compressive-force path' (CFP) [20], on the other hand, departs radically from the established design concepts, and seems to give an adequate and rational explanation of the behaviour of structural concrete. Design based on this concept has been applied successfully to RC [12,15,21] and PSC [22,23] statically determinate members made from a wide range of concrete strengths, resulting in economic and, above all, safer design solutions. The proposed method has also been found suitable in the design of indeterminate skeletal structures like RC continuous beams and fixed-ended portal frames [24].

The present paper aims at presenting further experimental evidence showing the suitability of the proposed (CFP) method in the design of PSC members. The load-carrying capacity, deformational response, fracture process and modes of failure of three PSC T-beams, having effective prestressing forces of about 60% of the ultimate strength of the prestressing tendons (designated here as type III PSC beams), have been examined in order to associate the causes and the mechanisms involved in their failure.

The type III PSC beams reported in this paper are very much similar to the type II PSC beams reported elsewhere [22]. The basic difference between these two types of beam is in the degree of prestressing. It is apparent from the code equations that the British Code, like any other code, gives quite an importance, in the design consideration, to the level of prestressing. If similar beams having different degrees of prestressing are designed to BS 8110, then the beams with lower amounts of prestressing would generally need greater amounts of shear reinforcement. In the modified compressive-field theory, the degree of prestressing is catered for by varying the angle θ (lower θ for higher prestressing). On the other

hand, the physical model proposed for the design of PSC members [14,22] (see below for details), in accordance with the concept of the CFP, takes care of the degree of prestressing by (a) shifting the location where the CFP changes its direction and (b) varying the amount of web reinforcement at these locations. For the type of PSC beams studied (under the adopted point-loading condition) the effect of the degree of prestressing on the amount of web reinforcement (as calculated by the CFP method) is, however, negligible for all practical purposes. The performance of types II and III PSC beams, designed either to BS 8110 or by the CFP method, have also been compared to monitor how the level of prestressing affects the behaviour of members designed by such methods.

2. PHYSICAL MODEL FOR PSC MEMBERS

The concept of the CFP is based on a proper understanding of concrete at the material level and thus provides a rational alternative for overcoming the deficiencies of present-day design thinking. On the basis of this concept, the load-carrying capacity of a structural concrete member is associated with the strength of concrete in the region of the paths along which compressive forces are transmitted to the support. The path of the compressive force may be visualized as a 'flow' of compressive stresses with varying section perpendicular to the path direction, the compressive force representing the resultant of the stresses at each section as shown in Fig. 2. Failure has been shown to be related to the presence of tensile stresses in the region of the path and such stresses may develop due to a number of causes, the main ones being associated with changes in the path direction, the varying intensity of the compressive stress field along the path, bond failure at the level of the tension reinforcement between two consecutive flexural inclined cracks, etc.

In contrast to RC members, a large amount of additional compressive force in the form of prestressing is available in a PSC member, and therefore such a prestressing force should play a vital role in determining the nature of the CFP. In Fig. 3 the 'frame-like' physical model developed for the design of PSC beams [22] is

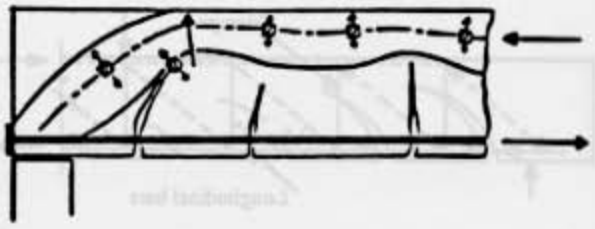

Fig. 2 Schematic representation of the compressive-force path.

shown. In this model, the length of the horizontal projection of the inclined leg of the compressive-force trajectory (h) has been considered to be primarily dependent upon the ratio of the amount of prestressing force (P_e) and the vertical reaction (R) at the support level. It is evident from the figure that, in a PSC beam, the inclined leg of the CFP at failure has been considered to take the direction of the force resultant at the support. The length h is therefore given by

$$h = (d - X_g) * P_e/R$$

where d is the effective depth of the beam and X_g is the distance of the centroid of the compression area from the top of the compression face. Unlike the case of RC beams, this simple relationship automatically takes care of the shear-span to depth (a/d) ratio, as the reaction R is a function of the a/d ratio (for a given flexural capacity). Although the model of Fig. 3 refers to PSC beams with a straight tendon profile, it can also be used for beams having inclined tendons [22]. It is important to note that shear reinforcement is only required in the region of the joint of the horizontal and inclined members of the frame with a nominal amount being sufficient in the remainder of the PSC beam. The shear reinforcement is designed so as to sustain the portion of the tensile force – balancing the action of the compressive forces acting along the members – that cannot be sustained by concrete alone.

A full description of CFP models for RC and PSC members, together with design examples and experimental verification is available elsewhere [12,14], where it has has been shown that the resulting design solutions are not only significantly more economical but also safer than

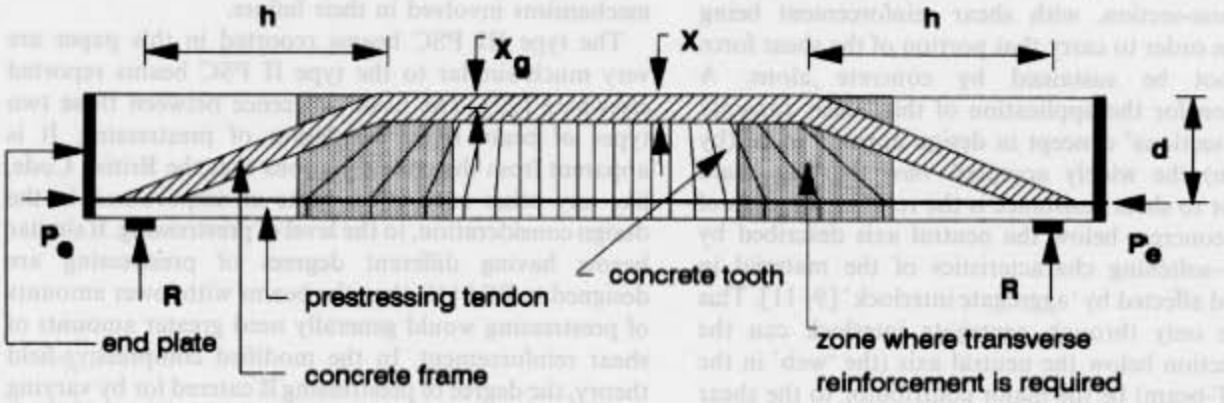

Fig. 3 Proposed frame model for prestressed concrete beam.

those obtained by using the methods recommended by current codes of practice. The relevant design details for beam PCB6 have been included in the Appendix.

3. EXPERIMENTAL PROGRAMME

The experimental work to be described here was intended not only to verify the accuracy of the proposed CFP physical model in the design of PSC members but also to demonstrate the inadequacy of the current shear design procedures. All the type III PSC T-beams tested in the present paper were initially prestressed to about 73.5% of the ultimate capacity of the prestressing tendons, with an effective prestressing force of about 60% of the strength of the strands. On the other hand, the type II PSC T-beams used previously [22] were initially prestressed to about 60% of the ultimate tendon capacity, with an effective prestressing force of about 50% of the failure load of the tendons.

3.1 Beam details

The type III PSC beams tested were 5660 mm long, simply supported with a span of 5000 mm and subjected to six-point loading. Typical cross-sectional characteristics and end-zone reinforcement details of the PSC beams studied are given in Fig. 4. The length of the T-section in the middle of the beam was 4000 mm. Beyond the T-section up to the end of the beam there was a rectangular section 200 mm wide × 300 mm high (see Fig. 4b). The web width of the T-section was only 40 mm. The widths of the top and bottom flanges of the beam section were 200 and 120 mm, respectively. The six-point loading configuration to which the beams were subjected is shown in Fig. 5.

The tensile reinforcement of the PSC beams comprised 12.9 mm diameter super steel strand wire conforming to BS 5896/3. Additional links and secondary reinforcement were provided in the flange of the beams; mild steel of 4 and 1.5 mm diameter was used for this purpose. The prestressing force in the post-tensioned beams under study was applied at the end face with the aid of two mechanical anchorages. The transition of this longitudinal compressive stress, from concentrated to uniformly distributed, produces transverse (vertical) tensile stresses which may lead to longitudinal cracking in the member. To prevent splitting and bursting, the end-zones of the beams were provided with additional reinforcement in the form of stirrup and longitudinal (Y8) bars (see Fig. 4c). Additional 8 mm diameter high-tensile steel bars were welded longitudinally to the end-plate to ensure that the latter component becomes an integral part of the beam when cast. Transverse reinforcement was provided by 1.5 mm diameter plain wire. Table 1 summarizes the strength characteristics of different bars and tendons used in this programme.

The design cube strength for the PSC beams was 55 MPa. In view of the very thin web and the difficulty involved in vibrating such a long beam, a superplasticizer

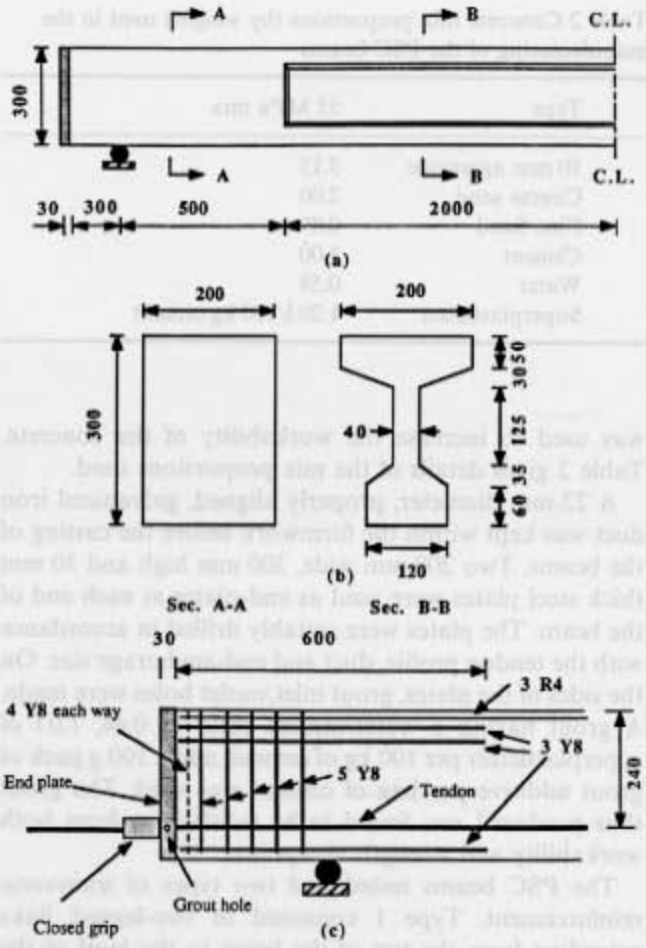

Fig. 4 (a, b) Cross-sectional characteristics and (c) reinforcement details of end-zones of the prestressed concrete beams tested in the programme (all dimensions and bar sizes are in mm).

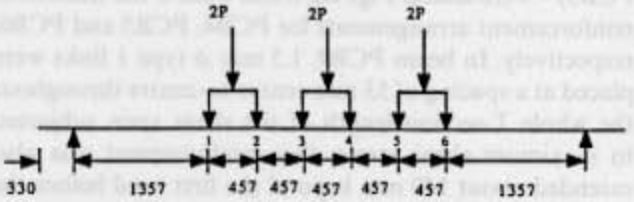

Fig. 5 Six-point loading configuration (all dimensions are in mm).

Table 1 Characteristics of reinforcement

Type of reinforcement	f_y (MPa)	f_u (MPa)
12.9 mm ϕ stabilized strand	–	1908.4
8 mm ϕ high-yield steel	470	565
4 mm ϕ mild steel	460	540
1.5 mm ϕ mild steel	460	510

Table 2 Concrete mix proportions (by weight) used in the manufacturing of the PSC beams

Type	55 MPa mix
10 mm aggregate	3.15
Coarse sand	2.00
Fine Sand	0.89
Cement	1.00
Water	0.58
Superplasticizer	1.20 l/100 kg cement

was used to increase the workability of the concrete. Table 2 gives details of the mix proportions used.

A 22-mm diameter, properly aligned, galvanized iron duct was kept within the formwork before the casting of the beams. Two 200 mm wide, 300 mm high and 30 mm thick steel plates were used as end-plates at each end of the beam. The plates were suitably drilled in accordance with the tendon profile, duct and end-anchorage size. On the sides of the plates, grout inlet/outlet holes were made. A grout having a water/cement ratio of 0.44, 1.01 of superplasticizer per 100 kg of cement, and a 100 g pack of grout additive per bag of cement was used. The grout thus produced was found to be satisfactory from both workability and strength viewpoints.

The PSC beams tested had two types of transverse reinforcement. Type 1 consisted of two-legged links extending from the top of the beam to the level of the prestressing tendon. Type 2 transverse reinforcement was a hoop-like reinforcement placed around the top flange of the beams.

Three type III PSC beams – one designed to BS 8110 (designated as PCB4), the second to the concept of the CFP (designated as PCB6), and the third one similar to PCB6 but without any web reinforcement (designated as PCB5) – were tested. Figs 6a, b and c show the transverse reinforcement arrangements for PCB4, PCB5 and PCB6, respectively. In beam PCB4, 1.5 mm ϕ type 1 links were placed at a spacing of 53 mm centre-to-centre throughout the whole T-section length of the shear span subjected to maximum shear stress; this reinforcement was also extended about 140 mm beyond the first (and before the sixth) load point. For the rest of the beam, type 1 links were placed at a spacing of 100 mm. Apart from these, and as recommended by BS 8110, type 3 reinforcement consisting of a straight piece of 4 mm ϕ mild steel was placed at the top of the top flange, perpendicular to the longitudinal direction of the beam at a spacing of 60 mm.

In beam PCB6, 1.5 mm ϕ type 1 reinforcement was placed at a spacing of 34 mm centre-to-centre for a distance $2d$ ($=480$ mm) at locations where the CFP changes its direction, in accordance with the physical model of Fig. 3 and following the recommendations of an earlier investigation [22]. Since the calculations have shown (see Appendix) that the centre of such locations is situated at a distance of 1100 mm from the supports, these links were placed at 240 mm on either side of that

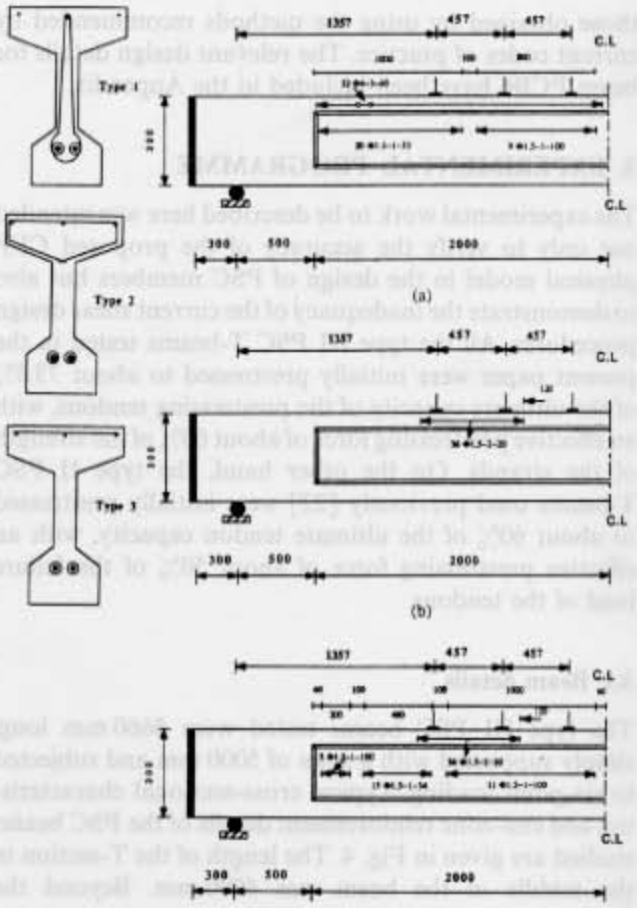

Fig. 6 Transverse reinforcement details of (a) PCB4, (b) PCB5 and (c) PCB6 (all dimensions and bar sizes are in mm).

spot. For the rest of the beam, nominal reinforcement as advocated by BS 8110, constituting 1.5 mm ϕ type 1 links at 100 mm spacing, was considered sufficient and was placed accordingly throughout that portion of the beam having a T-section. Type 2 reinforcement comprising 1.5 mm ϕ links was placed at a spacing of 20 mm from a distance of 120 mm before the first (and after the sixth) point-load to 120 mm after the second (and before the fifth) point-load.

The concrete strength characteristics of all these beams are given in Table 3. In the preliminary design calculation of the beams, 80% of the cube strength was assumed as the equivalent uniaxial cylinder compressive strength of the concrete. The actual cylinder strength was

Table 3 Concrete strength characteristics of the type III PSC beams tested

Beam	Time of testing (days)	Cube strength (MPa)		Cylinder strength on testing day (MPa)
		28 days	Testing day	
PCB4	79	53.4	58.1	45.4
PCB5	63	54.0	57.1	46.1
PCB6	75	54.3	57.8	45.7

Table 4 Predicted and measured load-carrying capacities of the type III PSC beams tested

Beam	Load type	Total sustained load (kN)			Failure type
		Predicted		Measured[a]	
		BS 8110	CFP		
PCB4	Six-point	92.18	–	93.0	Quasi-ductile
PCB5	Six-point	77.66	69.43	84.0	Brittle
PCB6	Six-point	85.34	92.18	92.5	Ductile

[a] Add weight of spreader beams (1.5 kN) to get total sustained load.

established on the day of testing. The detailed calculation regarding the assessment of web and flange reinforcement of all these beams is available elsewhere [14], while that of PCB6 may be found in the Appendix.

3.2 Prestressing and testing

The prestressing operation was carried out by means of a purpose-built rig (see elsewhere [14, 22] for details). Two identical 20-tonne jacks were energized together to stress both the tendons of the beams evenly. The prestressing process was monitored closely with the aid of several linear voltage differential transducers (LVDTs) and electrical resistance strain gauges. About one day after the completion of the prestressing exercise, the beams were re-prestressed and shims were inserted to cater for the losses due to slip at the jaws of the grips and due to initial relaxation. From the amount of final elongation of the tendons, the quantity of the initial prestressing force was calculated.

The six-point loading of the beams to failure was applied through three identical hydraulic jacks connected in series to a testing machine. Beneath every hydraulic jack, one spreader beam supported on two steel loading plates was placed. The midspan deflection, the 0.22 span deflection and the out-of-plane displacements were recorded. There were two LVDTs at the midspan, two on the sides to measure out-of-plane displacement and one LVDT at each of the 0.22 span locations from the support of the beam. At each load increment, the load was maintained constant for about 3 min in order to monitor the load and deformation response of the beam, mark the cracks (if any), and take photographs of the member's crack patterns.

The measured values of load, displacement and strain were recorded by a computer-logger capable of measuring to a sensitivity of ± 0.1 N, ± 0.0001 mm and ± 12 microstrains, respectively, with a speed of about 10 channels per second. Details of the prestressing, re-prestressing, grouting, loading, instrumentation, testing procedure and loading sequence, as well as the validation of the prestressing and testing set-ups, are available elsewhere [14].

4. DISCUSSION

4.1 Load-carrying capacity

In Table 4 the load-carrying capacities of PCB4, PCB5 and PCB6 have been listed. As can be seen from the table, both the British Code and the CFP concept predicted the load-carrying capacity of the PSC beams, designed by the respective methods, quite accurately. It should be stressed, however, that the total amount of web reinforcement in the maximum shear span of PCB6 was only about 65% of the web reinforcement of PCB4. The ratio of the amount of the web reinforcement present in the maximum shear span of type III PSC beams designed, respectively, to the CFP concept and BS 8110 was thus 0.65, matching fairly well the similar ratio of 0.60 that was found elsewhere [22] while studying type II PSC beams. The beam PCB4 failed in shear at an applied load of 93 kN (94.5 kN if the loads of the spreader beams are considered). On the other hand, the PSC beam PCB6 suffered a flexural failure at a total load (including spreader beams) of 94.0 kN.

The other conclusion that emerges from this investigation is that, although both methods could predict the ultimate load-bearing capacity of the beams with reasonable accuracy, the flexural failure load of PCB6 was about 15% less than that of the corresponding type II beam PCB2 having comparable cross-section and reinforcement details. One of the interpretations that can be put forward to justify these findings may be based on the effect of prestressing on the concrete strength. While, in the traditional way of thinking, it is usually assumed that an additional amount of prestressing naturally increases the concrete contribution to shear, such an increase in tendon force might well limit the capacity of concrete to carry additional compressive forces when it is subjected to live loading (since concrete is already loaded heavily due to the prestressing itself). It is worth recalling at this stage that it is the strength of the concrete through which the compressive force is transmitted, from the loading points to the supports, that determines, according to the proposed method, the strength of an RC or PSC member. Thus, PSC members, if heavily

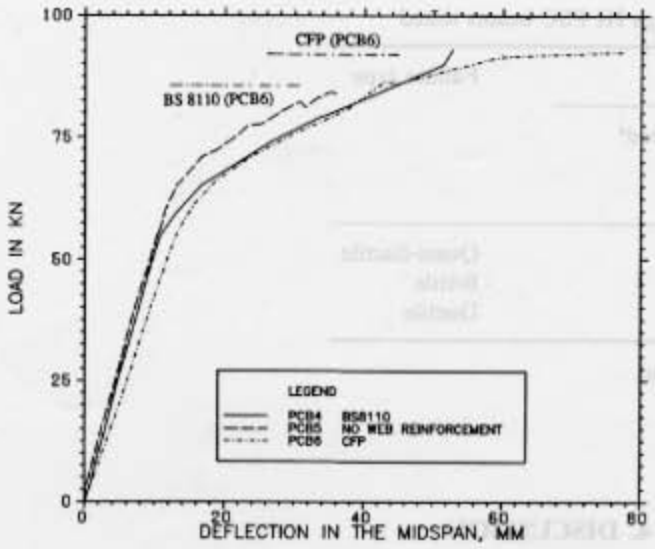

Fig. 7 Comparison of load–deflection curves of type III PSC beams tested in the programme.

prestressed, might fail at a load lower than a similar member with low prestress.

With regard to the somewhat poor prediction of the CFP concept in the case of PCB5, it may be mentioned that, while the calculated value has been obtained by assuming that there is no transverse reinforcement, the flange reinforcement has had a favourable effect (enhancing triaxiality) which, however, was ignored in the calculations. On the other hand, the underestimate of the British Code, although slightly smaller than its CFP counterpart, cannot be attributed to the presence of flange reinforcement as it does not subscribe to the notion that such reinforcement (being located above the neutral axis) can have any effect on the performance of such members.

4.2 Deformational response

Fig. 7 shows the load–deflection (P–δ) relationships obtained from the testing of the type III beams. The failure loads predicted by the British Code and the proposed method have been indicated in the same figure. The ductile nature of PCB6 is evident. In contrast, PCB4 had a quasi-ductile load–deflection curve. The response for PCB5 was brittle.

4.3 Cracking process

The cracking process of the PSC beam PCB4 can be described with reference to Fig. 8. The first set of flexural cracks were formed, in the bottom flange, at an applied load of about 65 kN. At 75 kN, and while these cracks were propagating more than half-way into the web, new diagonal cracks were formed in the adjoining regions. Additional shear cracks had formed by the time the applied load reached 80 N; most of the cracks reached the web–flange interface at this stage. As can be seen from the figure, upon reaching a load of 90 kN there was extensive diagonal cracking between the outer two pairs of load points. The beam failed at an applied load of about 93 kN when, all of a sudden, a diagonal crack penetrated deep into the flange near the midspan.

In Fig. 9 the crack patterns just before and after the failure of PCB5 are shown. The initial stages of the crack propagation of PCB5 were, on the whole, similar to those of PCB4. At the maximum sustained load of 84 kN, the 1357 mm long 'critical' shear span was free from any diagonal cracking. At failure (which took place when, after a pause of 2–3 min at the stable load of 84 kN, an attempt to increase the load further resulted in a sudden collapse with practically no load increase) the web, in the maximum-shear span, split longitudinally into two pieces, pointing to the requirement for vertical reinforcement to prevent this splitting.

The cracking process of PCB6 appears in Fig. 10. As for PCB4, the first set of flexural cracks was formed at an applied load of 65 kN. In the subsequent load steps, the flexural cracks increased both in number and in depth. From a load of 70 kN onwards, diagonally positioned shear cracks were formed. Like the case of beam PCB4, most of the diagonal and vertical cracks reached the web–flange interface at an applied load of 80 kN. Although additional shear cracks could be seen below the outermost loading points at a load of 90 kN, the number of such cracks was much smaller than in PCB4. The presence of the transverse flange reinforcement prevented the extension of inclined cracking into the flange of the beam. At an applied load of 92.5 kN, collapse eventually occurred due to failure of the compressive zone, right in the middle of the beam, between the innermost loading points.

4.4 Causes of observed behaviour and failure mechanism

It is apparent from the curves of Fig. 7 that the web reinforcement at locations where the CFP changes its direction played a vital role in the overall deformational behavior of the members. The basic difference in the performance of PCB4 and PCB6 was not the ultimate load-carrying capacity, but the ductility, which should be considered as an essential ingredient of a safe design method. Thus, even though the total amount of web reinforcement in PCB4 was larger than in PCB6, since it did not provide the necessary amount of transverse reinforcement at the change points of the CFP it could not sustain the tensile stresses developing at these locations. As a result, the web of PCB4 underwent more severe cracking (see Fig. 8) in comparison to PCB6 (see Fig. 10). Furthermore, in contrast to PCB6, beam PCB4 did not contain any link in the flange. Now, bond failure results in an increase in the length of the lever arm (Fig. 11), which in turn necessitates an enhancement in the average compressive strength of the concrete. Since the compression flange of PCB4 was not furnished with transverse reinforcement in the form of hoops, it was not capable of providing the confinement required for such

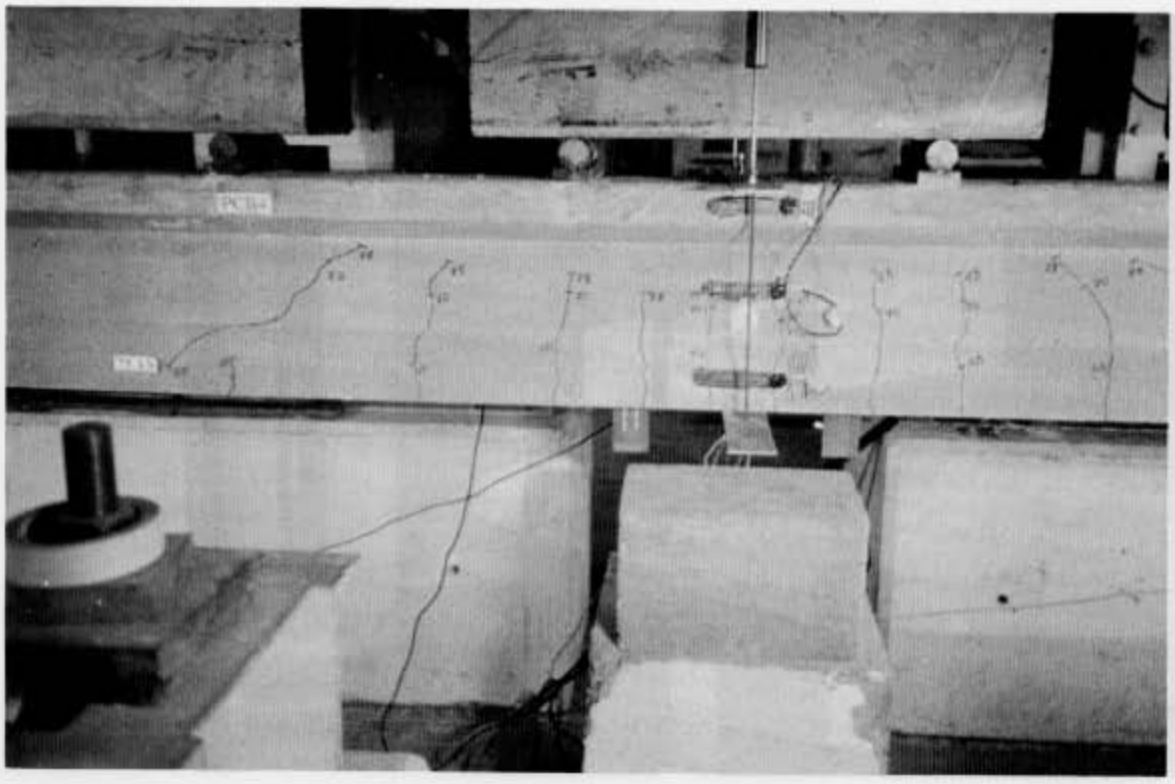

(a)

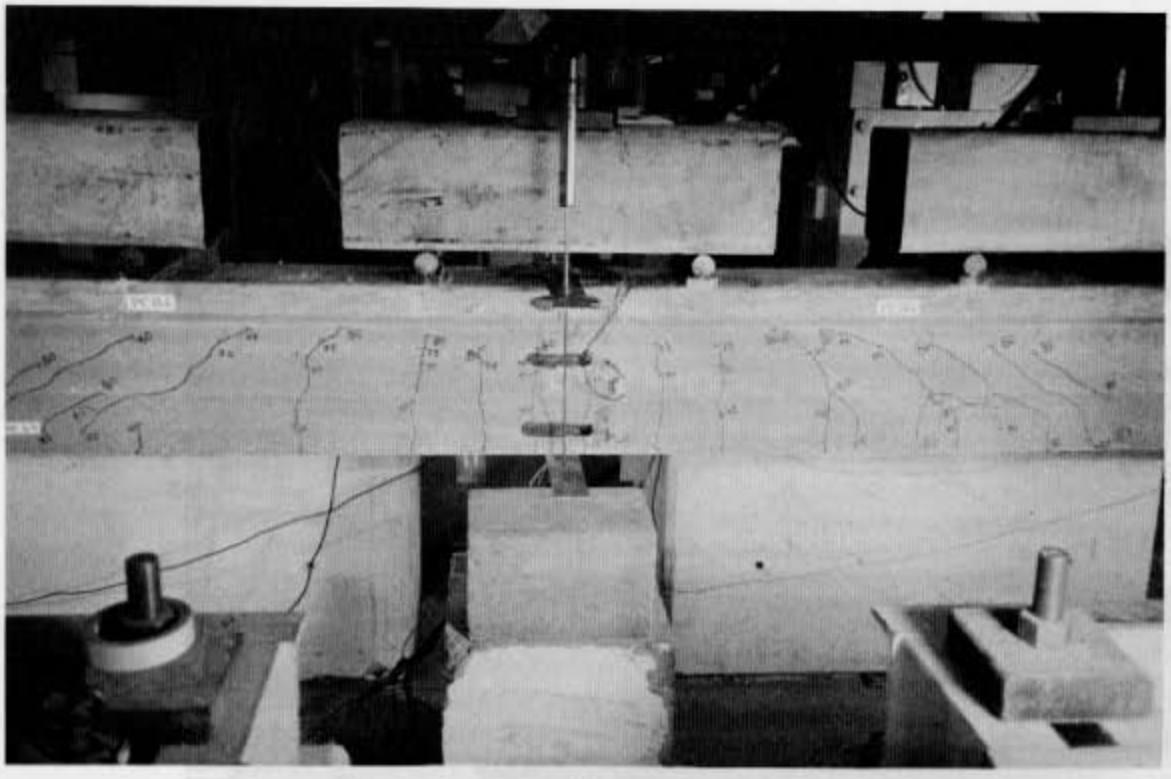

(b)

Fig. 8 Significant stages of the cracking process exhibited by PCB4 during its test to failure: (a) 75 kN, (b) 80 kN, (c) 90 kN, (d) failure at 93 kN.

(*continued*)

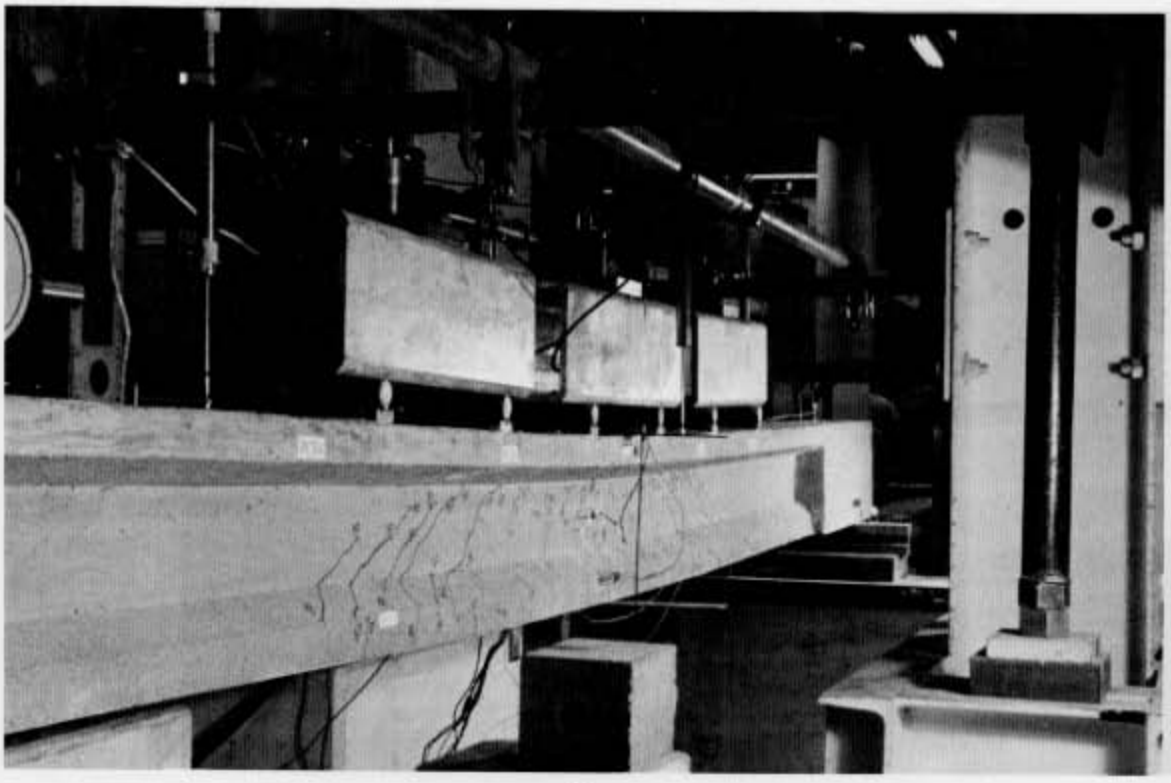

(c)

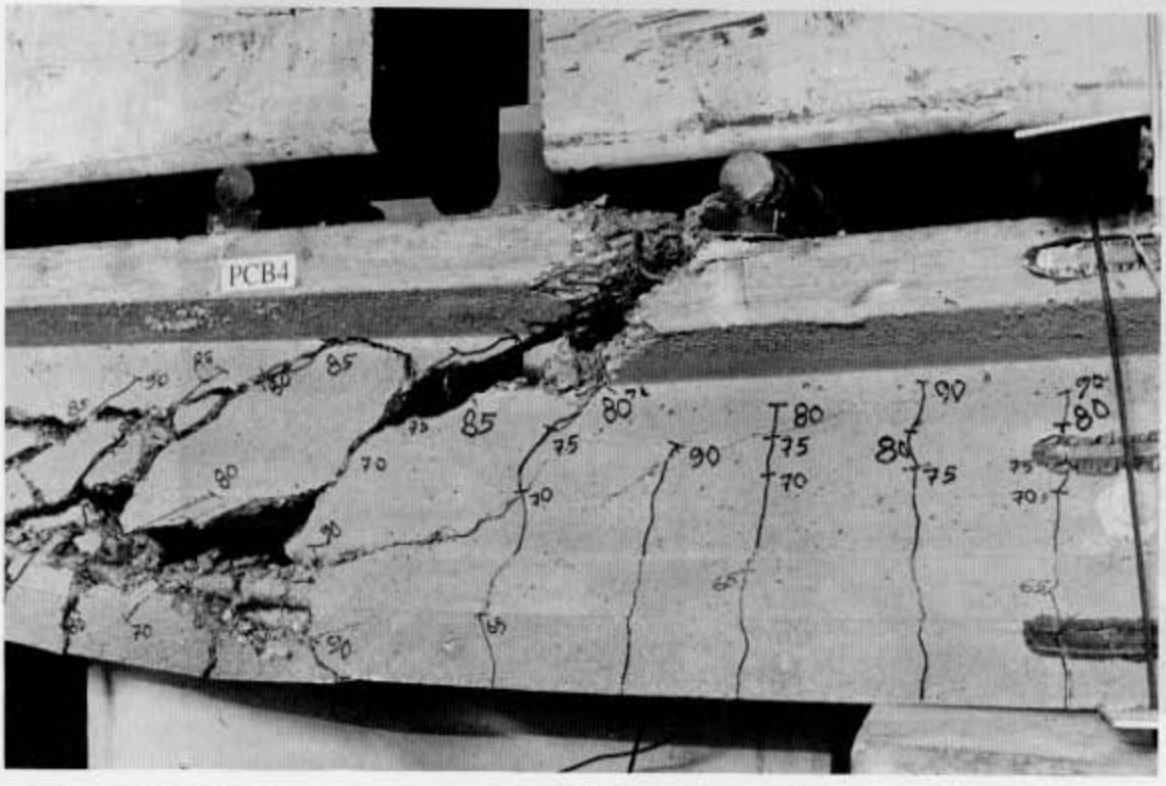

(d)

Fig. 8 (*continued*)

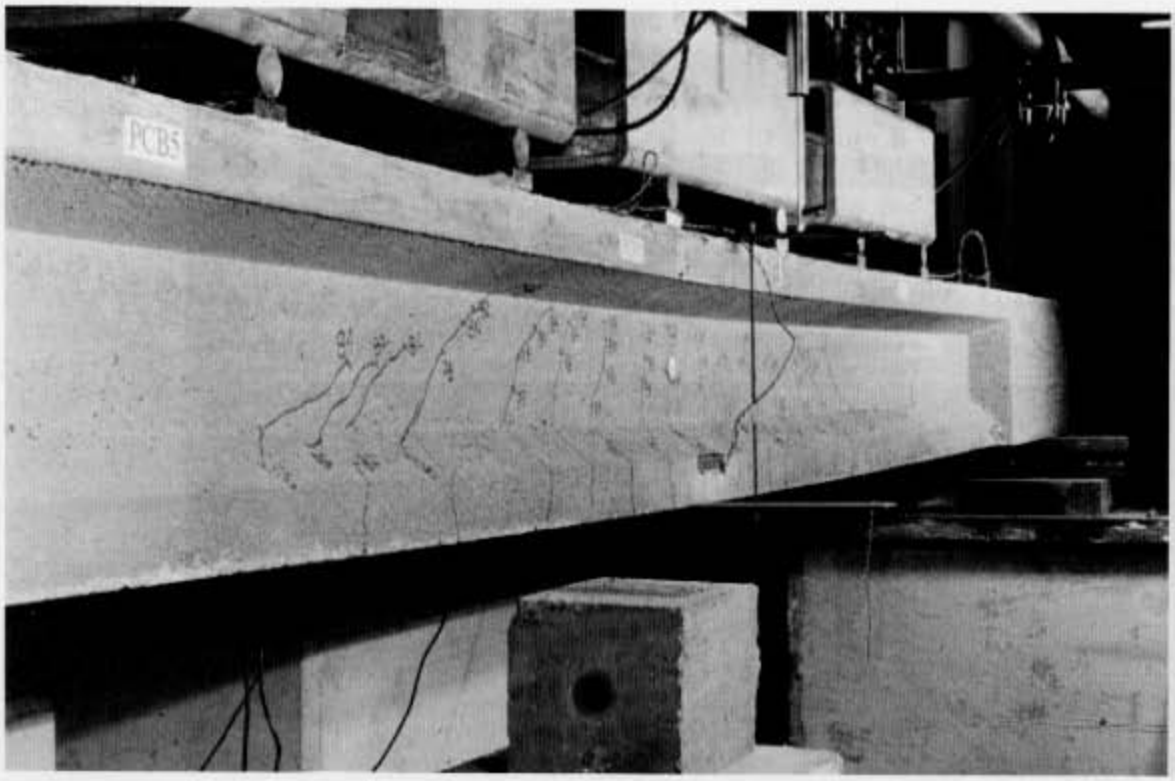

(a)

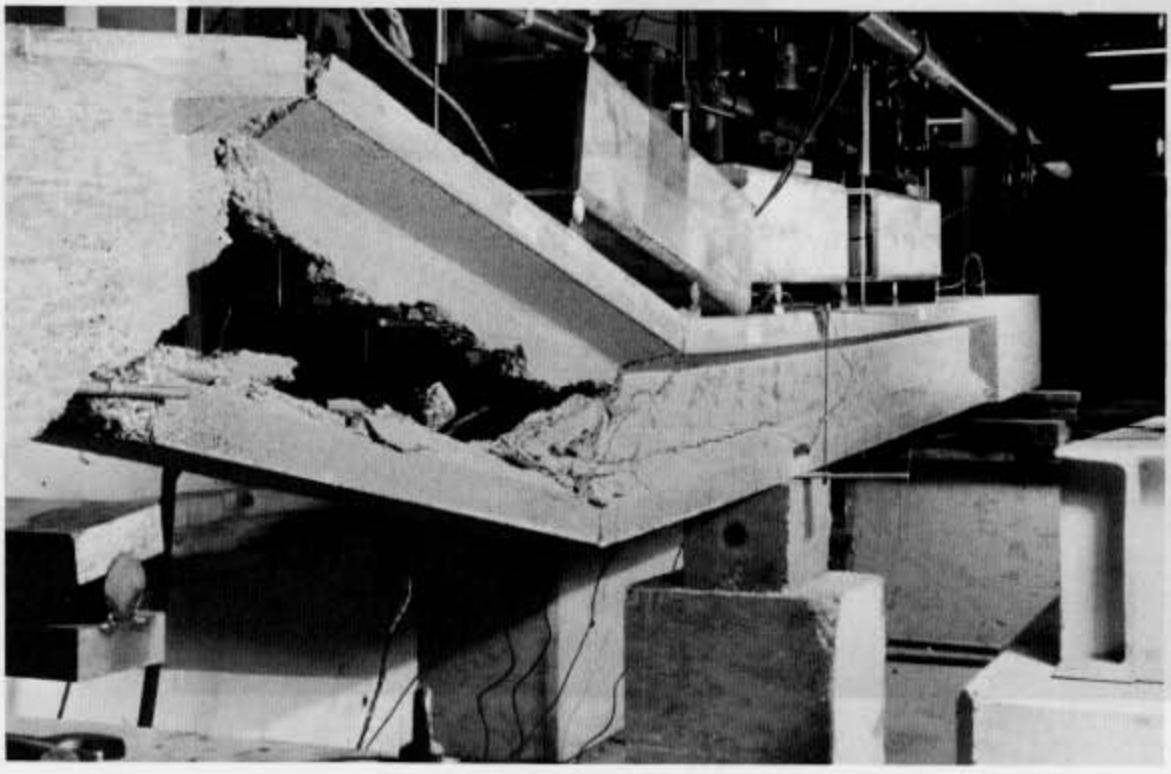

(b)

Fig. 9 Significant stages of the cracking process exhibited by PCB5 during its test to failure: (a) 84 kN, (b) failure at 84 kN.

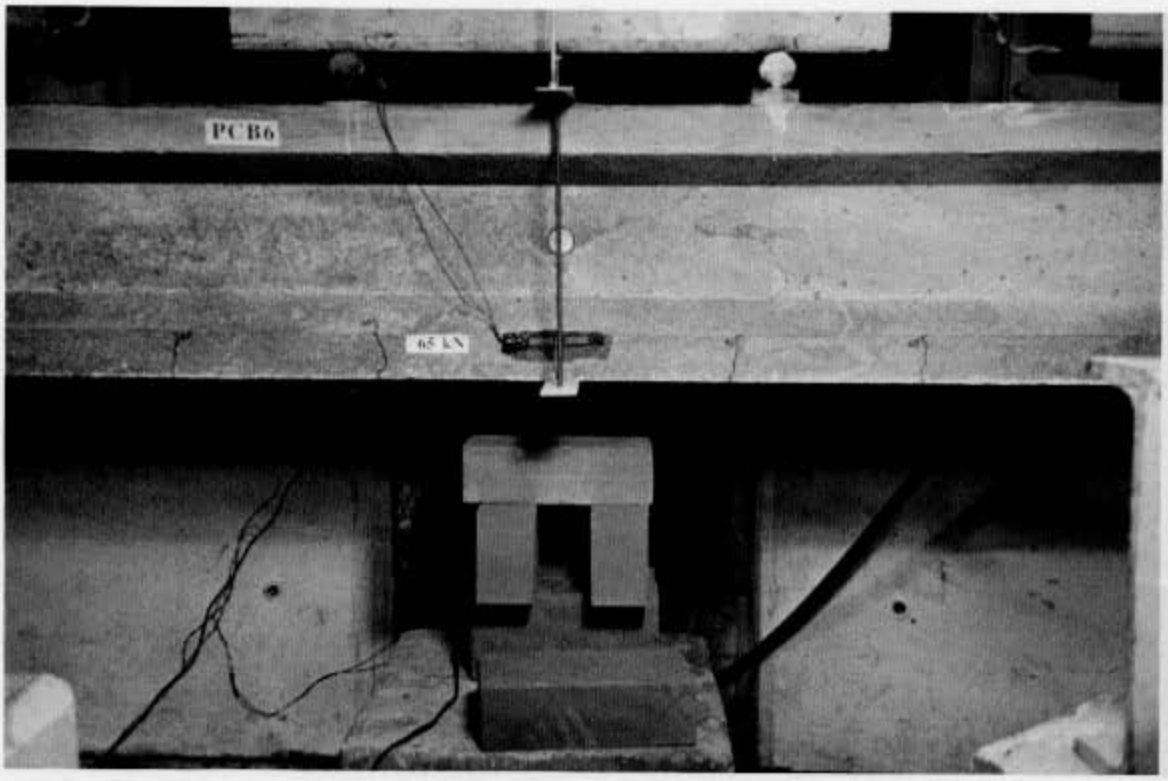

(a)

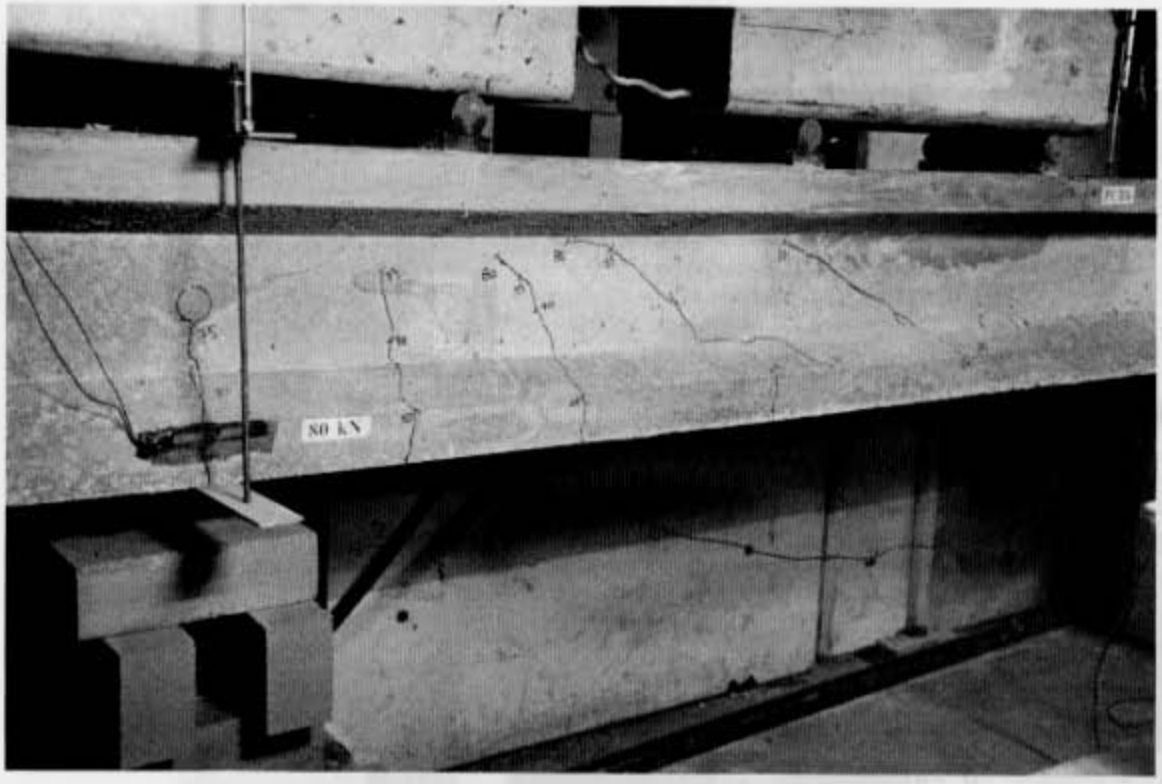

(b)

Fig. 10 Significant stages of the cracking process exhibited by PCB6 during its test to failure: (a) 65 kN, (b) 80 kN, (c) 90 kN, (d) failure at 92.5 kN, (e) failure zone at 92.5 kN.

(continued)

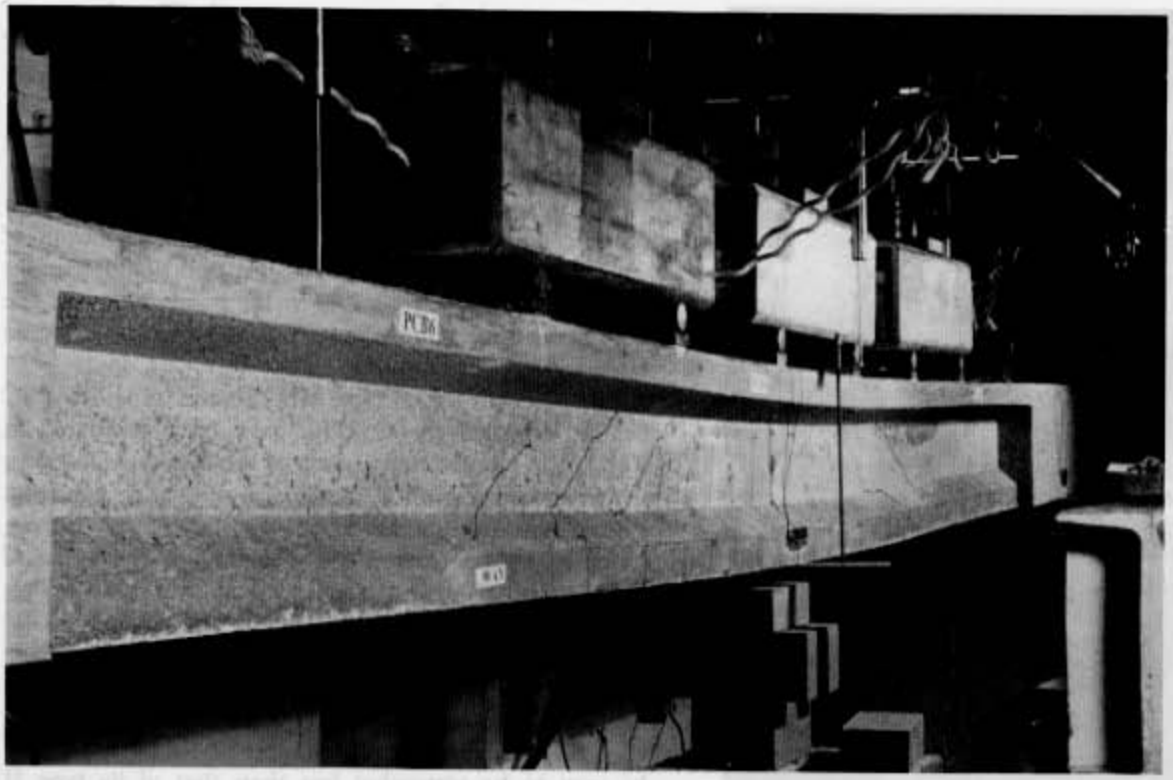

(c)

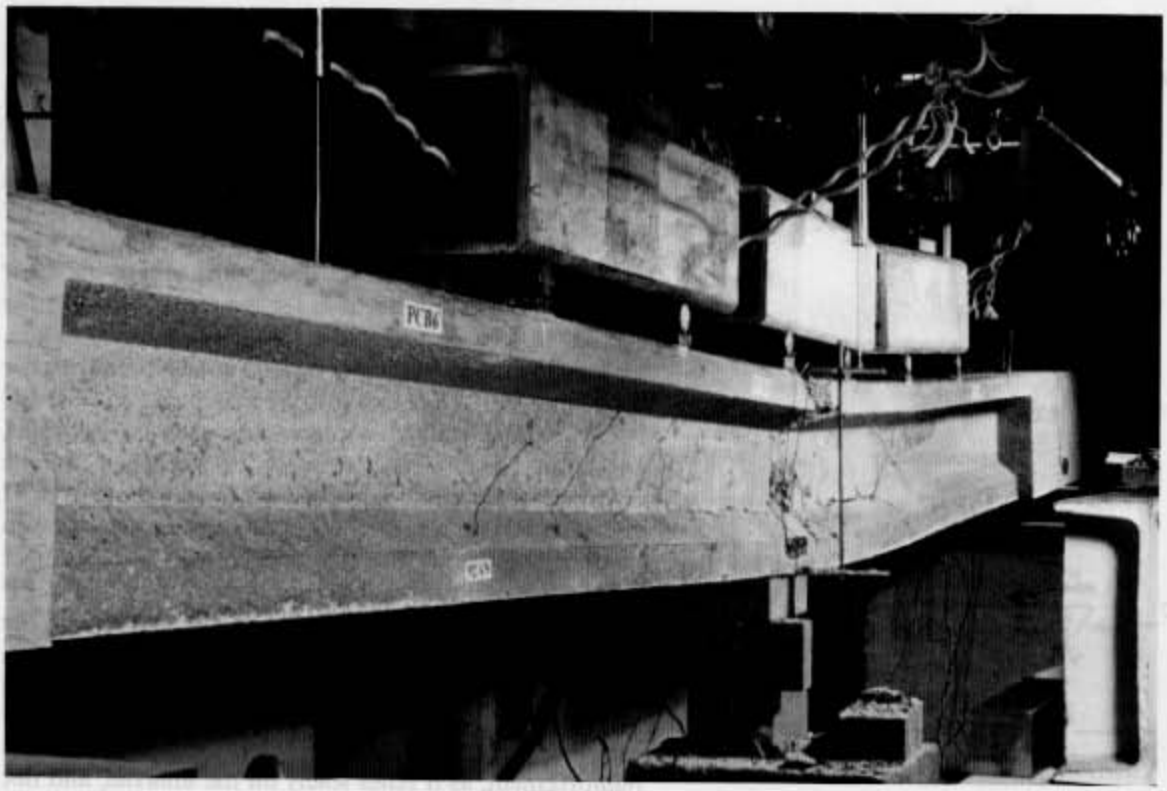

(d)

Fig. 10 (*continued*)

(*continued*)

(c)

Fig. 10 (*continued*)

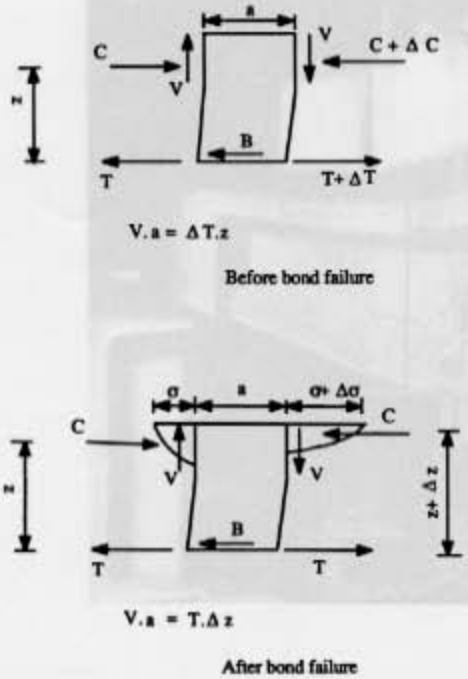

Fig. 11 Effect of bond failure on stress conditions in the compressive zone.

improvement in the concrete strength. The absence of such reinforcement allowed the sudden proliferation of cracks into the flange. Eventually, the PSC beam PCB4 failed in a quasi-ductile manner, as flange reinforcement usually contributes to the ductility of a reinforced concrete member [12]. In contrast, in the case of beam PCB6, the web was less severely cracked and the flange reinforcement prevented the abrupt propagation of cracks into the flange that possible bond failure might produce. It is, therefore, due to the combination of the above-mentioned causes that PCB6 experienced a ductile failure.

The P–δ curves of type II [22] and type III PSC beams, designed to BS 8110, have been compared in Fig. 12a. A similar comparison of the beams designed to the proposed (i.e. CFP) method is shown in Fig. 12b. Fig. 12a shows that the initial legs of the P–δ curves, obtained by comparing the deformation responses of PCB3 and PCB4, are almost identical. Due to the higher amount of prestress, this initial branch for PCB4 terminated at a higher load. After this primary branch, the P–δ curves of both the above beams turn at an angle and continuing propagating upwards, almost in parallel straight lines. The ductility of type III beam PCB4 may be seen to be somewhat less than that of its type II counterpart, PCB3. In contrast to the beams designed to the BS 8110, the P–δ curves of the PSC beams designed to the proposed CFP method are not bilinear. The initial straight portions of the curves turn gradually into a ductile, roughly horizontal, branch. The more severely prestressed PCB6 shows a little less ductility than PCB2. From this exercise, the effect of increasing the amount of prestressing may be seen to diminish the total amount of deflection and ductility. It is apparent that, in a PSC member, provision of reinforcement according to the CFP concept, using the physical model described in Fig. 3, results in safer design solutions than the presently available code provisions. The CFP method catered not only for the tensile stresses developing where the CFP changes its direction but also for the (additional) tensile stresses that developed in the flange due to bond failure. In keeping with the observations made in an earlier investigation [22], it can also be concluded that 'truss' behaviour is neither a necessary, nor a sufficient, condition for a PSC member to undergo ductile deformational behaviour; the PSC beams (both type II and type III) designed to BS 8110 contained more web reinforcement (and, thereby, transformed into stronger 'trusses' after shear cracks were formed) than their CFP counterparts, and yet failed in an unsafe manner. On the other hand, the beneficial effect of the 'localized design transverse reinforcement' in the web of the CFP beams cannot be explained by means of the truss model. Nor can the truss model account for the role of flange reinforcement, as it relies solely on the uniaxial, and not multiaxial, stress–strain relationship of concrete; in this respect, the nominal (0.4%) straight-bar reinforcement (perpendicular to the longitudinal direction) in the flanges advocated by BS 8110 (see Fig. 6a) goes some

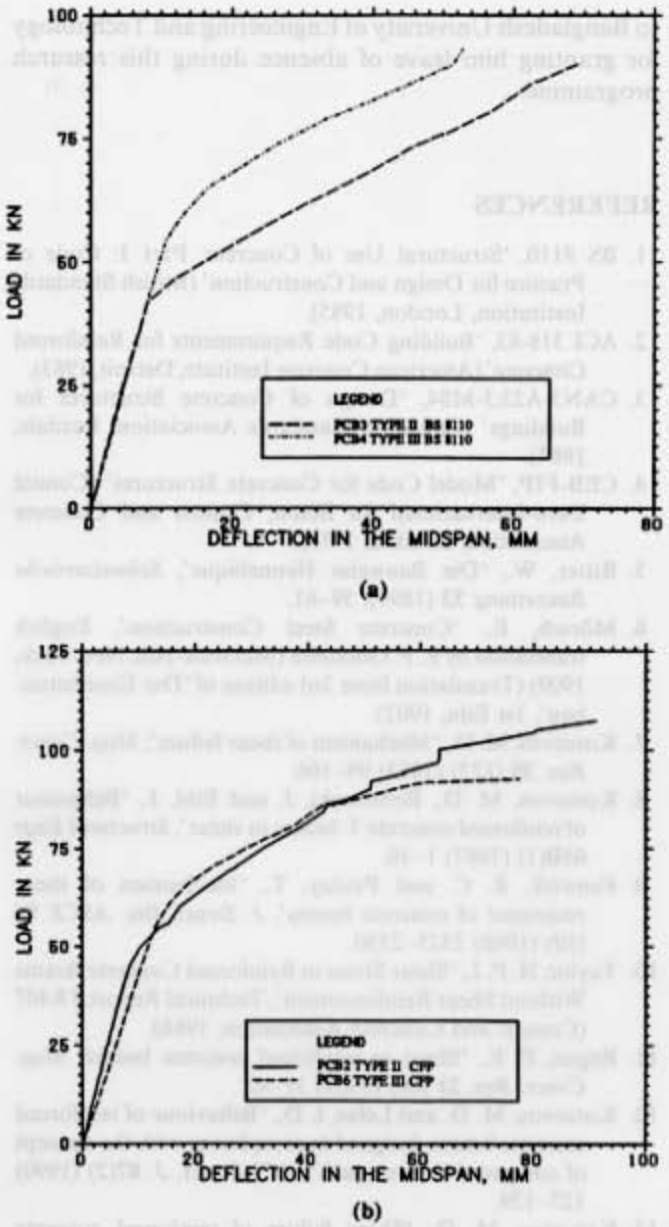

Fig. 12 Comparison of load–deflection curves of type II and type III PSC beams designed to (a) BS 8110 and (b) CFP methods.

way towards delaying tensile cracks due to triaxial effects, although the latter effects do not form part of this code's rationale.

5. Conclusions

1. Although the beams designed to the CFP concept and the British Code failed almost at the same load (and agreed well with the calculated values), the load–deformational behaviour of the beam designed to the CFP model was much more ductile than that of its BS 8110 counterpart. This ductility, being achieved by using about 35% less web reinforcement than the other beam, shows that design based on realistic physical models can be economical, as well as safer.

2. The flexural failure loads of type III PSC beams were found to be smaller than the values obtained from the experimentation of similar type II PSC beams. It is possible that concrete elements in the compressive zone of type III beams, being already subjected to higher stresses due to the larger amount of prestressing in comparison to similar type II PSC beams, reach the ultimate (triaxial) failure stress envelope earlier. Consequently, the failure load becomes smaller. This, in contrast to the current way of thinking, indicates that an additional amount of prestressing, instead of increasing the shear contribution of concrete, may, in fact, limit the load-bearing capacity of the member itself.

APPENDIX: CFP method design calculations for PCB6

A1. Flexural capacity (see Fig. 4)

$A_s = 205.4\ \text{mm}^2$ and $f_u = 1908.4\ \text{N mm}^{-2}$ gives $T = 391\,985.3$ N.

$f_{cu} = 55\ \text{N mm}^{-2}$ gives $\sigma_c = 0.67 f_{cu} = 36.85\ \text{N mm}^{-2}$.

Since $C = T$, $A_c = 391\,985.3/36.85 = 10\,637.32\ \text{mm}^2$.

Thus $X = 53.5$ mm and $X_g = 26.67$ mm.

Lever arm $z = 240 - 26.67 = 213.33$ mm.

Hence flexural capacity $M_f = 391\,985.3 \times 213.33 = 83\,621\,580$ N mm.

Maximum total sustained six-point load as indicated in Fig. 5 is $6 \times 15\,361.73$ N.

A2. Shear force sustained by concrete

Shear span $s = 1357.5$ mm ($> 2d = 480$ mm).

According to the CFP method [12,14], the moment corresponding to the failure load (in N mm) is given by

$$M_c = 0.875sd\left[0.342b_1 + 0.3\frac{M_f}{d^2}\left(\frac{z}{s}\right)^{1/2}\right]\left(\frac{16.66}{\rho_w f_y}\right)^{1/4} \quad \text{(A1)}$$

where the various parameters are defined in the Notation and in Fig. A1.

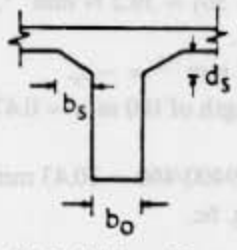

Fig. A1 Definition of b_1 used in Equation A1 .

The tensile force that can be resisted by concrete alone in the region where the path changes its direction (in N) is given by

$$V_c = M_c/s \quad \text{(A2)}$$

Using Equations A1 and A2, $M_c = 47\,128\,960$ N mm and $V_c = 34\,717.47$ N.

Applied bending moment at $s = 1357.5$ mm, $M_a = 62\,561\,140$ N mm $> M_c$.

Thus shear reinforcement is required. The location around which the compressive-force path will change its direction can be determined with the aid of the proposed model of Fig. 3.

Initial prestressing force $P_i = 0.735T = 288\,109.3$ N.

Considering 18% losses, effective prestressing force $P_e = 0.82P_i = 236\,249.6$ N.

Thus $h = (d - X_g)P_e/R = (240 - 26.67)236\,249.6/46\,085 = 1094$ mm $\simeq 1100$ mm.

A3. Transverse reinforcement

(i) For excess tension due to change in path direction [12, 14]

$T_{sv} = V_a - V_c = 46\,085.19 - 34\,717.47 = 11\,367.72$ N.

$A_{sv} = (V_a - V_c)/f_{yv} = 11\,367.72/460 = 24.71$ mm^2.

Provide $8\phi 1.5$–1–34, as shown in Fig. 6c.

(ii) For excess tension due to bond failure (Fig. A2)

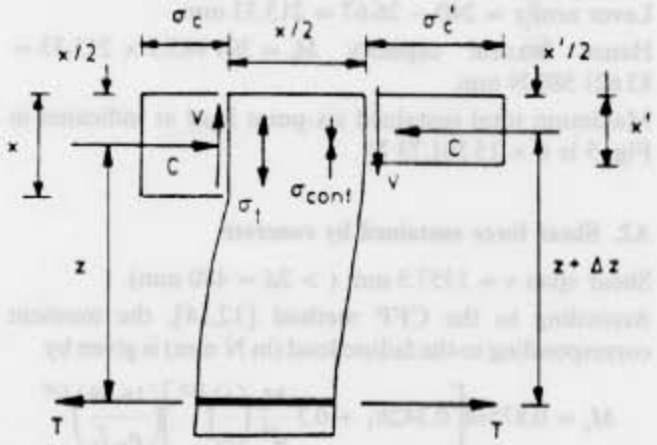

Fig. A2 Assessment of excess tension due to bond failure.

$\Delta z = (V_a - V_c)X/2T = (46\,085.19 - 34\,717.47)53.5/(2 \times 391\,985.3) \simeq 1$ mm.

$x' = 2(d - z - \Delta z) = 2(240 - 213.33 - 1) = 51.34$ mm.

$\sigma_c' = C/(bx') = 391\,985.3/(200 \times 50) = 39.2$ N mm^{-2}, omitting the tapered part.

$\sigma_{conf} = (\sigma_c' - 0.8f_{cyl})/5 = 0.47$ N mm$^{-2} = -\sigma_t$.

Tensile stress resultant over a length of 100 mm $= 0.47 \times 200 \times 100 = 9400$ N.

Required reinforcement is $A_{sv} = 9400/460 = 20.43$ mm^2.

Use $\phi 1.5$–2–20, as shown in Fig. 6c.

ACKNOWLEDGEMENTS

The authors owe their thanks to the Science and Engineering Research Council, UK for financing the experimental work reported in this paper. The first author would like to express his gratitude to the Association of Commonwealth Universities, UK, for awarding him a Commonwealth Scholarship to carry out research of which the present work forms part. Thanks are also due to Bangladesh University of Engineering and Technology for granting him leave of absence during this research programme.

REFERENCES

1. BS 8110, 'Structural Use of Concrete: Part 1: Code of Practice for Design and Construction' (British Standards Institution, London, 1985).
2. ACI 318-83, 'Building Code Requirements for Reinforced Concrete' (American Concrete Institute, Detroit, 1983).
3. CAN3-A23.3-M84, 'Design of Concrete Structures for Buildings' (Canadian Standards Association, Rexdale, 1984).
4. CEB-FIP, 'Model Code for Concrete Structures' (Comité Euro-International du Béton, Cement and Concrete Association, London, 1978).
5. Ritter, W., 'Die Bauweise Hennebique', *Schweizerische Bauzeitung* **33** (1899), 59–61.
6. Mörsch, E., 'Concrete Steel Construction', English translation by E. P. Goodrich (McGraw-Hill, New York, 1909) (Translation from 3rd edition of 'Der Eisenbetonbau', 1st Edn, 1902).
7. Kotsovos, M. D., 'Mechanism of shear failure', *Mag. Concr. Res.* **35** (123) (1983) 99–106.
8. Kotsovos, M. D., Bobrowski, J. and Eibl, J., 'Behaviour of reinforced concrete T-beams in shear', *Structural Engr* **65B**(1) (1987) 1–10.
9. Fenwick, R. C. and Paulay, T., 'Mechanism of shear resistance of concrete beams', *J. Struct. Div. ASCE* **94** (10) (1968) 2325–2350.
10. Taylor, H. P. J., 'Shear Stress in Reinforced Concrete Beams Without Shear Reinforcement', Technical Report TR407 (Cement and Concrete Association, 1968).
11. Regan, P. E., 'Shear in reinforced concrete beams' *Mag. Concr. Res.* **21** (66) (1969) 31–42.
12. Kotsovos, M. D. and Lefas, I. D., 'Behaviour of reinforced concrete beams designed in compliance with the concept of compressive force path', *ACI Struct. J.* **87**(2) (1990) 127–139.
13. Kotsovos, M. D., 'Shear failure of reinforced concrete beams', *Eng. Struct.* **9**(1) (1987) 32–38.
14. Seraj, S. M., 'Reinforced and Prestressed Concrete Members Designed in Accordance to the Compressive-Force Path Concept and Fundamental Material Properties', Ph.D. thesis, Imperial College, University of London (1991).
15. Seraj, S. M., Kotsovos, M. D. and Pavlović, M. N., 'Behaviour of high-strength mix reinforced concrete beams', submitted for publication.
16. Kotsovos, M. D. and Pavlović, M. N., 'Non-linear finite element modelling of concrete structures: basic analysis, phenomenological insight and design implications', *Eng. Computns* **3**(3) (1986) 243–250.
17. Collins, M. P., 'Towards a rational theory for RC members in shear', *J. Struct. Div. ASCE* **104**(4) (1978) 649–666.
18. Vecchio, F. J. and Collins, M. P., 'The modified compression-field theory for reinforced concrete elements subjected to shear', *ACI Struct. J.* **83**(2) (1986) 219–231.
19. Schlaich, J., Schäfer, K. and Jennewein, M., 'Toward a consistent design of structural concrete', *Prestr. Concr. Inst. J.* **32**(3) (1987) 74–150.

20. Kotsovos, M. D., 'Compressive force path concept: basis for reinforced concrete ultimate limit design', *ACI Struct. J.* **85**(1) (1988) 68–75.
21. Lefas, I. D., Kotsovos, M. D. and Ambraseys, N. N., 'Behaviour of reinforced concrete structural walls: strength, deformation characteristics, and failure mechanisms', *ibid.* **87**(1) (1990) 23–31.
22. Seraj, S. M., Kotsovos, M. D. and Pavlović, M. N., 'Experimental study of the compressive-force path concept in prestressed concrete beams', submitted for publication.
23. *Idem*, 'Nonlinear finite-element analysis of prestressed concrete members', *Struct. & Buildings, Proc. ICE* **94** (4) (1992) 403–418.
24. *Idem*, 'Application of the compressive-force path concept in the design of reinforced concrete indeterminate structures: A pilot study', submitted for publication.

RESUME

Chemin de compression et comportement de poutres de béton précontraint

L'étude des codes actuels montre assez clairement qu'en dépit d'un réel effort de recherche, une compréhension vraiment rationnelle et complète du béton structurel nous fait encore défaut. On peut en trouver une raison dans notre peu d'intelligence du matériau. A ce propos, l'utilisation d'équations de calcul courant repose sur des concepts et/ou des théories qui s'appuient invariablement sur des caractéristiques de contrainte–déformation uniaxiales (plutôt que triaxiales).

Les règles de calcul sont basées de préférence sur des équations de calcul plutôt que sur des modèles réalistes. On dispose, bien sûr, de modèles physiques, mais la plupart ne semblent guère valables. On présente ici une étude de la performance de poutres de béton précontraint calculées soit conformément à des méthodes conventionnelles, soit grâce à un modèle physique conforme au concept de 'chemin de compression' qui stipule que la résistance d'un élément de béton structurel est associée à la résistance du béton à proximité du chemin le long duquel les forces de compression se transmettent. C'est en notant la présence de contraintes multiaxiales dans un élément de béton armé ou précontraint, en reconnaissant que le béton est un matériau fragile, et en constatant les imperfections du 'modèle en treillis' traditionnel et de 'l'enchevêtrement de granulat' qu'on en est venu à introduire le concept de 'chemin de compression'.

Les résultats d'essais sur des poutres lourdement chargées montrent que les éléments calculés suivant ce concept peuvent présenter une sécurité supérieure à leurs équivalents obtenus d'après les codifications. On a comparé le comportement de ces poutres avec celui de poutres similaires (également calculées suivant les dispositions des codes ou selon la méthode préconisée) – mais soumises à un taux de précontrainte inférieur – afin de contrôler l'influence du niveau de précontrainte sur le comportement d'éléments calculés d'après différentes méthodes. Il ressort, contrairement à la manière de voir habituelle, qu'une augmentation de la précontrainte, au lieu d'accroître la résistance au cisaillement du béton, peut, en fait, limiter la capacité portante de l'élément même.